Journal of
Mechanical
Science and
Technology

Journal of Mechanical Science and Technology 21 (2007) 2117~2124

Influence of support viscoelastic properties on the structural wave propagation

Junhong Park*

School of Mechanical Engineering, Hanyang University, 17 Haengdang-dong, Seongdong-gu, Seoul, 133-791, Korea

(Manuscript Received July 11, 2007; Revised August 27, 2007; Accepted August 28, 2007)

Abstract

The dissipation of the structural vibration energy at viscoelastic supports is an efficient method of reducing modal resonances and consequent noise and fatigue related problems. The support stiffness has significant impact on the modal characteristics. The dissipation capabilities of the viscoelastic support depend on its stiffness. Methods to optimally tune this support stiffness are proposed in this study. The characteristic mechanical impedance for structural vibration is obtained from wave propagation analysis and non-reflecting boundary conditions. The wave propagation is analyzed near the supports installed at edges, middle of a structure, and for the tuned vibration absorber. The dependence of the optimal stiffness on the location and mass of the supports is identified. A simple analytical solution for optimal support stiffness for maximum dissipation of propagating vibration energy at supports is presented.

Keywords: Viscoelastic supports; Wave propagation; Vibration control; Optimal support stiffness; Structural vibration

1. Introduction

Damping is an efficient method for reducing the noise and vibration response of structures. It does not require external hardware to actively control and monitor the responses. To enhance the damping in the structures, it is not always possible to add damping in the structure itself. An alternative approach is to control vibration via viscoelastic supports. For dissipation of structural vibration, the viscoelastic materials are widely used as the supporting material. The modal properties and sound radiation characteristics are affected by the support stiffness especially at low frequencies. Among the modal parameters, modal damping, which is the index showing the capability of vibration reduction, is determined by elastic and inelastic properties of the supports. The approach of optimally tuning the support stiffness is attractive since the mechanical properties of the supports are easier to modify than those of the supported structure itself.

Many vibration control methods have been proposed for continuous systems. In particular, dynamic absorbers have been used to reduce the vibrations of continuous systems such as rods and beams [1]. Dynamic absorbers consist of a mass, spring, and viscous damper attached to the primary structure. Optimal values for the absorber natural frequency and damping ratio must be calculated to minimize the vibrations of specific modes at resonances. For plates and shells, the dynamic absorber performance was analyzed by using the receptance method [2].

In cases where structures are compliantly supported, the support mass is often negligible relative to that of the supported structure. The support may be idealized as a stiffness along the boundaries. The effects of support flexibility on the vibration of beams and plates have been investigated before. Kang and Kim [3] investigated the effects of support stiffness on the vibration of beams and plates. The flexible supports were represented by translational and rotational

*Corresponding author. Tel.: +82 2 2220 0424, Fax.: +82 2 2298 4634
E-mail address: parkj@hanyang.ac.kr

springs with complex stiffnesses. The variation of the modal properties of the structures with the support stiffness was calculated. Macbain and Genin [4] developed numerical methods using a central difference formula to analyze the vibrations of beams with flexible supports. The system loss factors were found to increase with a decrease in the support-to-beam elastic modulus ratio. Chen and Zhou [5] investigated the effects of damping on the vibrations of distributed systems using wave propagation methods. Forced vibration response and sound radiation of the compliantly supported classical plate were investigated by Park et al. [6]. The optimal stiffness that minimized the forced vibration and sound radiation from a rectangular plate was obtained from the Rayleigh-Ritz method and wave propagation analysis. The optimal values obtained from the two different methods agreed well with each other.

In this study, the wave propagation near compliant supports is analyzed to calculate the optimal support properties for minimal vibration response. The compliant supports are idealized as distributed translational and rotational spring, inertia and damping elements. Reflection ratios are calculated from the relationship between incident waves to reflected and transmitted waves. From the non-reflecting boundary condition which is impedance matched supports, the characteristic mechanical impedance for structural vibration is obtained and compared to the case of simple longitudinal vibration. The supports are assumed to be located at the edges and at the middle of the structure. The theoretical methods to calculate the optimal support stiffness that minimizes the velocity response of the structure are presented.

2. Characteristic mechanical impedance – a vibrating solid bar

The mechanical impedance defined as force over velocity is widely used to characterize the response of a mechanical system to external excitations. For a mass, m, supported by a spring with stiffness s_t, Fig. 1(a), the mechanical impedance is estimated as

$$\hat{Z} = \frac{\hat{F}}{i\omega\hat{w}} = i\left(m\omega - \frac{s_t}{\omega}\right). \tag{1}$$

The usual complex notation is used, $F(t)$= $\mathrm{Re}\{\hat{F}e^{i\omega t}\}$. From the information of the mechanical impedance, the time- or frequency-dependent response of the system to external loads is calculated. When the damping in the system is neglected, the mechanical impedance calculated from Eq. (1) is purely imaginary. This implies that the energy input from the external loads is stored as the kinetic and potential energy of the system or reflected back to the source.

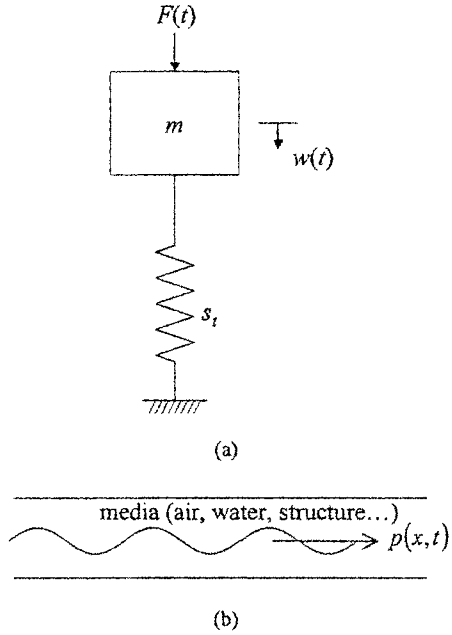

Fig. 1. (a) A rigid mass supported by a spring, (b) wave propagation in a continuous system.

For continuous systems, Fig. 1(b), such as plates, membranes, beams, and fluids, the wave propagation is a fluctuation of force (or pressure) and velocity of the media over space and time. With this propagation, the vibrational energy transfers over space, which causes resonance if the system has a finite size. Since the wave propagation is the simultaneous fluctuation of force and velocity over space and time, two quantities are related to each other, and cannot be specified independently. The characteristic mechanical (or acoustic) impedance defines the relationship between the force and the velocity. For example, the relationship between the pressure and the particle velocity for the plane traveling sound waves in air is $\hat{p}/\hat{v} = \rho_a c$, where ρ_a is the air density and c is the speed of sound. In this case, $\rho_a c$ is the characteristic acoustic impedance. Contrary to the mechanical impedance shown in Eq. (1), the characteristic mechanical or acoustic impedance is purely real if the damping in the media is negligible, which implies that the energy input from

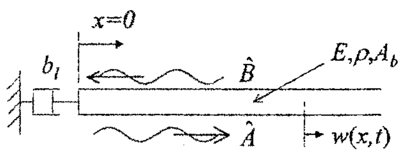

Fig. 2. Longitudinal wave propagation near the boundary of a solid bar.

external loads propagate over space if the size of a media is infinite.

The following example, a vibrating solid bar, shows that complete absorption of the incident waves occurs when the boundary impedance matches the characteristic impedance. For the quasi-longitudinal wave propagation of the sold rods, the wave equation is [7],

$$\frac{\partial^2 w}{\partial x^2}+\frac{\rho}{E}\frac{\partial^2 w}{\partial t^2}=0\,, \tag{2}$$

where E is Young's modulus and ρ is the density. For the longitudinal wave propagation, the wave speed, $c=\sqrt{E/\rho}$, does not depend on the frequency (non-dispersive wave propagation). The characteristic impedance in this case is $\rho c=\sqrt{\rho E}$. For the wave reflection at x=0 in Fig. 2, the ratio between the amplitudes of the incident, B, and reflected waves, A, is calculated by applying the boundary condition at x=0:

$$E\frac{\partial \hat{w}(0)}{\partial x}=\left(ib_l\omega\right)\hat{w}(0)\,. \tag{3}$$

The coefficient b_l is the boundary impedance, $b_l=\hat{p}(x=0)/(i\omega\hat{w}(x=0))$ where $\hat{p}$ is the amplitude of the fluctuating stress of the longitudinal wave. The solution of Eq. (3) is assumed as

$$\hat{w}(x)=\hat{A}e^{-ikx}+\hat{B}e^{ikx}\,, \tag{4}$$

where A and B are the complex amplitudes of the reflected and the incident harmonic waves, respectively, and k is the wave number. From Eqs. (3) and (4), the reflection ratio for the wave propagation shown in Fig. 2 is obtained as

$$\frac{\hat{A}}{\hat{B}}=\frac{E-cb_l}{E+cb_l}\,. \tag{5}$$

Note that the longitudinal wave speed does not depend on the frequency, and consequently the characteristic acoustic impedance ($\rho c=\sqrt{\rho E}$) is also frequency-independent. From Eq. (5), there is no reflection of the propagating waves, i.e., A=0, when the boundary impedance matches the characteristic acoustic impedance, $b_l=\sqrt{\rho E}$. This suggests that the complete absorption of the incident waves occurs when the boundary impedance matches the characteristic impedance of the longitudinal wave propagation, thereby minimizing the undesirable vibration of the rod.

The wave propagation analysis at the boundary of the solid rod shown in this section is a simple example demonstrating the numerical procedures to obtain the boundary condition that induces the maximum dissipation of the incident waves. In Eq. (4), the assumed displacement includes only propagating wave terms. This approach equally applies to systems with second order differential equation of motions similar to Eq. (2), for example, vibrating strings, torsional and shear vibration of rods. When the differential equation of motion is fourth order, for example a compliantly supported rectangular plate, similar approaches are used for the vibration analysis as described in the following section.

3. Wave propagation analysis of the vibrating structure

3.1 Wave propagation at the edge of the classical plate

In this session, transverse waves approaching normally to the edge are considered. The plate is assumed to be infinitely long in the x-direction in order to allow for the calculation of the reflection ratio of the normally incident bending waves. Transverse displacements are assumed to vary only with the distance along the direction normal to the edge. Fig. 3(a) illustrates the wave propagation at the edge and middle of the plate. The equation of motion for the free transverse vibrations of a homogeneous plate without any constraints in the y-direction is [7],

$$D\frac{\partial^4 w}{\partial x^4}+\rho h\frac{\partial^2 w}{\partial t^2}=0, \tag{6}$$

where $D = Eh^3/12(1-\nu^2)$ is the bending stiffness, w is the transverse displacement for flexural vibration, h is the thickness, and ν is Poisson's ratio. For the trans-

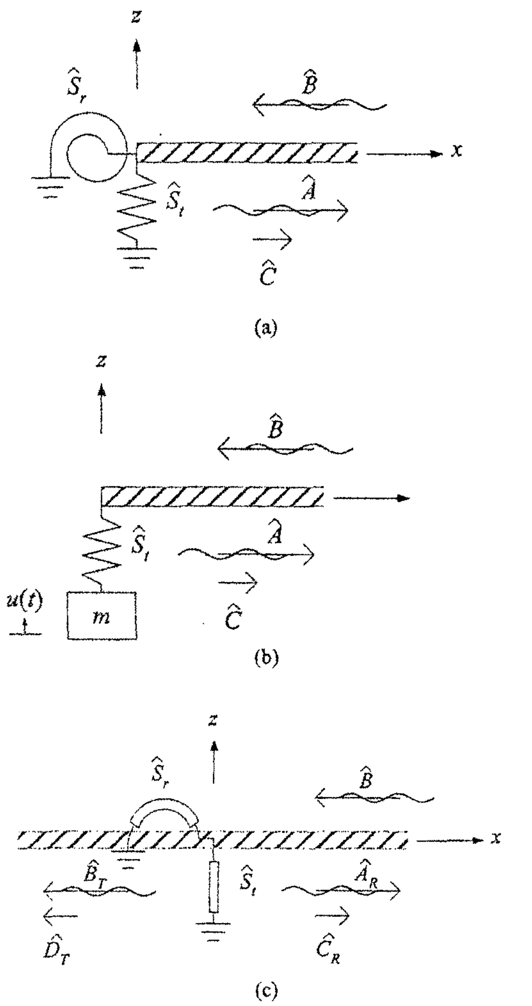

Fig. 3. Wave propagations (a) at the edge, (b) at the vibration absorber, and (c) at the middle of a structure, when the incident wave with complex amplitude $\hat{B}$ approaches from $x=\infty$.

verse vibration, the wave speed, $c_b = \left(\omega^2 D/\rho h\right)^{1/4}$, increases with increasing frequency. To determine the wave propagation characteristic at the edge, two boundary conditions are applied as

$$D\frac{\partial^3 \hat{w}(0)}{\partial x^3} = -\hat{S}_t \hat{w}(0), \quad D\frac{\partial^2 \hat{w}(0)}{\partial x^2} = \hat{S}_r \frac{\partial \hat{w}(0)}{\partial x}, \tag{7a,b}$$

where $\hat{S}_t$ and $\hat{S}_r$ are the translational and rotational boundary stiffnesses, respectively. Normally incident harmonic waves with complex amplitude $\hat{B}$ are assumed to propagate toward the edge from $x = \infty$. The plate displacement is expressed as

$$\hat{w}(x) = \hat{A}e^{-ik_b x} + \hat{B}e^{ik_b x} + \hat{C}e^{-k_b x}, \tag{8}$$

where k_b is the bending wave number related to the circular frequency, $k_b = \left(\omega^2 \rho h/D\right)^{1/4}$. Applying the boundary conditions, Eq. (7), the transfer functions between the incident and reflected harmonic waves are obtained as [6]

$$\frac{\hat{A}}{\hat{B}} = \frac{(i+1)+2i\hat{R}-2\hat{T}-(i+1)\hat{R}\hat{T}}{(i-1)+2i\hat{R}+2\hat{T}-(i-1)\hat{R}\hat{T}}, \quad \frac{\hat{C}}{\hat{B}} = \frac{2i\left(1+\hat{R}\hat{T}\right)}{(i-1)+2i\hat{R}+2\hat{T}-(i-1)\hat{R}\hat{T}}, \tag{9a,b}$$

where the non-dimensional parameters are defined as:

$$\hat{T} = \frac{\hat{S}_t}{Dk_b^3}, \quad \hat{R} = \frac{\hat{S}_r}{Dk_b}. \tag{10a,b}$$

3.1.1 Viscous supports

From the wave propagation analysis, the characteristic mechanical impedance of structure is identified from non-reflecting boundary conditions. To investigate non-reflecting boundary conditions, viscous supports are considered. The non-dimensional stiffness parameters are given as

$$\hat{T} = \frac{i\omega b_t}{Dk_b^3}, \quad \hat{R} = \frac{i\omega b_r}{Dk_b}. \tag{11a,b}$$

From Eqs. (9) and (11), the non-reflecting boundary condition is satisfied when the damping coefficients are

$$b_t = \frac{Dk_b^3}{\omega}, \quad b_r = \frac{Dk_b}{\omega}. \tag{12a,b}$$

These coefficients are identical to the characteristic mechanical impedances of the transversely vibrating plate [6]. The plate supports must include both translational and rotational viscous damping elements for non-reflecting boundary conditions. In contrast with the characteristic acoustic impedance of a vibrating solid rod, which is frequency independent, the characteristic translational and rotational impedances of transversely vibrating plates depend on frequency.

3.1.2 Viscoelastic supports

For viscoelastically supported plates, the support stiffness is composed of complex translational and rotational springs. The non-dimensional boundary stiffnesses are given by

$$\hat{T} = T(1+i\eta_t) = \frac{S_t}{Dk_b^3}(1+i\eta_t),$$
$$\hat{R} = R(1+i\eta_r) = \frac{S_r}{Dk_b}(1+i\eta_r), \tag{13a,b}$$

where S_t and S_r are the real parts of the complex support stiffnesses, and η_t and η_r are the loss factors. By substituting Eq. (13) into Eq. (9), the reflection ratios are calculated in terms of T, R, η_t, and η_r. For the viscoelastically supported case, the non-reflecting boundary condition that induces complete dissipation of reflected waves of amplitudes A and C does not occur. However, a support stiffness that minimizes the amplitude of reflected propagating bending waves can be found. The exponentially decaying waves have a limited influence, and only at the edges. This component does not contribute to the resonance. They are neglected in the calculation. Only the reflected propagating waves with complex amplitudes are minimized in the optimization problem. The minimum reflection occurs when the parameters of the boundary stiffnesses satisfy the equations:

$$\frac{\partial|\hat{A}/\hat{B}|^2}{\partial T} = 0, \quad \frac{\partial|\hat{A}/\hat{B}|^2}{\partial R} = 0,$$
$$\frac{\partial|\hat{A}/\hat{B}|^2}{\partial \eta_t} = 0, \quad \frac{\partial|\hat{A}/\hat{B}|^2}{\partial \eta_r} = 0. \tag{14a-d}$$

When the plate is supported by translational springs only (R=0), the real part and the loss factor of the optimal translational stiffness for minimum reflection of propagating waves are obtained as, from Eqs. (14 a, c),

$$S_{t,opt} = \frac{k_b^3 D}{2}, \ \eta_{t,opt} = 1. \tag{15a,b}$$

The corresponding reflection ratio is zero, which suggests that complete absorption of incident vibrational energy can occur. However, the loss factor in Eq. (15) is greater than typical loss factor value of many viscoelastic materials, which is usually less than 0.3 [8]. For constant loss factor, the optimal support stiffness is obtained from Eq. (14a) as,

$$S_{t,opt} = \frac{k_b^3 D}{\sqrt{2(1+\eta_t^2)}}. \tag{16}$$

3.2 Tuned vibration absorber

A same approach is expanded to include the mass in the support system, as shown in Fig. 3(b). When the mass of the support system is considered after neglecting the rotational stiffness, the support becomes the tuned vibration absorber. The mass attached to the support stiffness increases the vibration energy dissipation due to the resonance of the support system, itself. There are many different approaches to optimally tune the parameters of the tuned vibration absorber. In this study, the wave propagation approach following the same procedures as for the viscoelastic supports is used to find the optimal parameters. The three boundary conditions for Fig. 3(b) are:

$$\frac{\partial^3 \hat{w}(0)}{k_b^3 \partial x^3} = -\hat{T}(\hat{w}(0) - \hat{u}), \tag{17a-c}$$
$$\frac{\partial^2 \hat{w}(0)}{\partial x^2} = 0, \quad -\hat{M}\hat{u} = \hat{T}(\hat{w}(0) - \hat{u}),$$

where $M = m\omega^2/Dk_b^3$ and u is the displacement of the mass. Consequently, the following transfer function matrix is obtained:

$$\begin{bmatrix} (i+\hat{T}) & (-1+\hat{T}) & -\hat{T} \\ -1 & 1 & 0 \\ \hat{T} & \hat{T} & (\hat{M}-\hat{T}) \end{bmatrix} \begin{bmatrix} \hat{A} \\ \hat{C} \\ \hat{u} \end{bmatrix} = \begin{bmatrix} (i-\hat{T}) \\ 1 \\ -\hat{T} \end{bmatrix} \hat{B}. \tag{18}$$

Using Eq. (18) the reflection at the edge which is supported by the vibration absorber is obtained as:

$$\frac{\hat{A}}{\hat{B}} = \frac{(i+1)(M-T) - 2TM}{(i-1)(M-T) + 2TM},$$
$$\frac{\hat{C}}{\hat{B}} = \frac{2i(M-T)}{(i-1)(M-T) + 2TM}, \tag{19a-c}$$
$$\frac{\hat{U}}{\hat{B}} = \frac{-4iT}{(i-1)(M-T) + 2TM}.$$

If the mass becomes infinity (M=∞) the reflection ratios are obtained exactly same as those of the viscoelastic supports as expected. If the damping in the absorber is neglected, then the magnitude of the incident wave is equal to that of the reflected waves. Only the phase of the reflected wave changes. Using Eq. (18), the effects of viscous or viscoelastic support stiffness can be analyzed. The parameters of the tuned vibration absorber to be determined are m, S_t, and η_t.

As an example, the tuned vibration absorber consisting of the mass and viscoelastic stiffness is considered. In the analysis to find the optimal properties, the amplitudes of the decaying waves and vibration of the attached mass (C and U, respectively) are neglected. Fig. 4 shows the calculated dissipation ratio (=1- $|\hat{A}/\hat{B}|^2$). The loss factor was assumed to be constant (η_t=1). The parameters that maximize this dissipation ratio minimize the reflection from the vibration absorber and are determined as the optimal properties. Note that maximum dissipation of vibration occurs when the non-dimensional parameters are close to unity, i.e., $M = m\omega^2/Dk_b^3 \approx 1$ and $T = S_t/Dk_b^3 \approx 1$. The same numerical procedures can be repeated for different values of the loss factor, and also for the supports consisting of viscous damper and elastic springs following the same numerical procedures.

3.3 Wave propagations in the middle of the classical plate

For some applications, compliant supports may be installed in the middle of the structure. One practical example is the belt line seal that supports the vehicle window. Also, beam or ring stiffeners may be added to the plate to enhance the stiffness with minimum amount of added material, which is important for minimizing the weight and increasing the fuel efficiency of vehicles. In such cases, the rotational and translational impedance includes loadings from stiffeners, elastic supports, and distributed or lumped masses. All these loadings can be included as shown in Fig. 3(c), and the complex impedance is now expressed as

$$\hat{S}_t = \frac{\hat{F}(0)}{\hat{w}(0)} = \hat{S}_t' - \omega^2 m_t, \quad \hat{S}_r = \frac{\hat{T}(0)}{\hat{\theta}(0)} = \hat{S}_r' - \omega^2 I_r, \tag{20a,b}$$

where m_t is the mass and I_r is the polar moment of inertia of the stiffener and the mass attached to the structure. Note that $\hat{S}_t'$ and $\hat{S}_r'$ are the complex impedance defined in section 3.1. As a generalization of the complex stiffness in this section, $\hat{S}_t$ and $\hat{S}_r$ include the inertia loading. With the wave propagations shown in Fig. 3(c), the plate displacement is given as

$$\hat{w}(x) = \left(\hat{A}_R e^{-ik_b x} + \hat{B} e^{ik_b x} + \hat{C}_R e^{-k_b x}\right) H(x) + \left(\hat{D}_T e^{k_b x} + \hat{B}_T e^{ik_b x}\right)\left(1 - H(x)\right), \tag{21}$$

where H is the Heaviside step function. In Eq. (21), there are five unknown amplitudes. By applying four boundary conditions at x=0, the reflection and transmission ratios near the compliant supports are estimated. The four boundary conditions at x=0 are:

$$\hat{w}(0^+) = \hat{w}(0^-), \quad \frac{\partial \hat{w}}{\partial x}(0^+) = \frac{\partial \hat{w}}{\partial x}(0^-), \tag{22a,b}$$

$$D\left(\frac{\partial^3 \hat{w}(0^+)}{\partial x^3} - \frac{\partial^3 \hat{w}(0^-)}{\partial x^3}\right) = -\hat{S}_t \hat{w}(0),$$

$$D\left(\frac{\partial^2 \hat{w}(0^+)}{\partial x^2} - \frac{\partial^2 \hat{w}(0^-)}{\partial x^2}\right) = \hat{S}_r \frac{\partial \hat{w}(0)}{\partial x}. \tag{22c,d}$$

By replacing Eq. (21) into Eq. (22), the following transfer function matrix is obtained:

$$\begin{bmatrix} 1 & 1 & -1 & -1 \\ i & 1 & i & 1 \\ i+\hat{T} & \hat{T}-1 & i & -1 \\ i\hat{R}-1 & \hat{R}+1 & 1 & -1 \end{bmatrix} \begin{Bmatrix} \hat{A}_R \\ \hat{C}_R \\ \hat{B}_T \\ \hat{D}_T \end{Bmatrix} = \begin{bmatrix} -1 \\ i \\ i-\hat{T} \\ 1+i\hat{R} \end{bmatrix} \hat{B}, \tag{23}$$

where the non-dimensional stiffness parameters, T and R, are defined in Eq. (13). From Eq. (23), the following transfer functions are calculated.

$$\frac{\hat{A}_R}{\hat{B}} = \frac{2\hat{T} - 2\hat{R} + \hat{R}\hat{T}}{-8i + 2(i-1)\hat{T} - 2(i+1)\hat{R} + i\hat{R}\hat{T}},$$

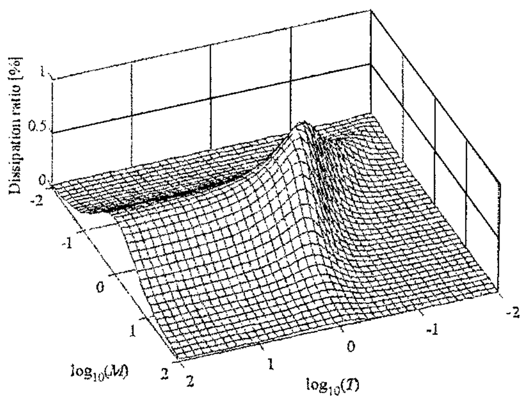

Fig. 4. Dependence of reflection ratio on the parameters of the tuned vibration absorber (mass and stiffness) assuming constant loss factor.

$$\frac{\hat{C}_R}{\hat{B}} = \frac{-2i\hat{T} + 2\hat{R} - (i+1)\hat{R}\hat{T}}{-8i + 2(i-1)\hat{T} - 2(i+1)\hat{R} + i\hat{R}\hat{T}}, \quad \text{(24a,b)}$$

$$\frac{\hat{B}_T}{\hat{B}} = \frac{2i(\hat{T} - 4 - \hat{R})}{-8i + 2(i-1)\hat{T} - 2(i+1)\hat{R} + i\hat{R}\hat{T}},$$

$$\frac{\hat{D}_T}{\hat{B}} = \frac{2(i\hat{T} + \hat{R})}{-8i + 2(i-1)\hat{T} - 2(i+1)\hat{R} + i\hat{R}\hat{T}}. \quad \text{(24c,d)}$$

For the above reflection and transmission coefficients, complete dissipation of the incident wave with complex amplitudes, B, occurs when the impedances have the following values:

$$\hat{S}_t = (2-2i)Dk_b^3, \ \hat{S}_r = (-2-2i)Dk_b. \quad \text{(25a,b)}$$

Unlike the case of the support stiffness at the edge, physical implementation of Eq. (25) is not straightforward, since the loss factors are negative. When the loss factor is negative, the harmonic displacement response should occur earlier than the input force, which is not possible for passive elements. Consequently, the complete dissipation of incident wave at the support does not occur when the support is purely viscoelastic. Instead, the support impedance that minimizes the reflection or transmission of propagating waves is calculated in the following. To minimize the number of variables and by following the discussion in section 3.1.2, the loss factors are assumed to be fixed.

When the support stiffness is purely translational, the ratio of the reflected and transmitted propagating waves to the incident wave is obtained as, from Eq. (24),

$$\left|\frac{\hat{A}_R}{\hat{B}}\right|^2 + \left|\frac{\hat{B}_T}{\hat{B}}\right|^2 = \frac{T^2 + (T-4)^2 + 2T^2\eta^2}{(-4 + T(1-\eta))^2 + T^2(1+\eta)^2}. \quad \text{(26)}$$

The maximum dissipation of the incident propagating wave can occur when

$$\frac{\partial\left(\left|\frac{\hat{A}_R}{\hat{B}}\right|^2 + \left|\frac{\hat{B}_T}{\hat{B}}\right|^2\right)}{\partial T} = 0. \quad \text{(27)}$$

The optimal translational support stiffness that induces maximum dissipation of incident wave is consequently obtained as:

$$S_{t,opt} = \sqrt{\frac{8}{(1+\eta_t^2)}}k_b^3 D. \quad \text{(28)}$$

Note that the optimal stiffness calculated from Eq. (28) is exactly four times larger than the stiffness that induces maximum dissipation of the incident waves at the edge, Eq. (16). Fig. 5(a) shows the reflection ratio calculated by using Eq. (26). There is only one absolute minimum for each loss factor value. The minimum value depends on the value of the loss factor similarly to the case of the supports at the edge.

The numerical procedures are repeated for the plate supported by the rotational viscoelastic elements in the middle. The optimal rotational support stiffness that induces maximum dissipation of incident wave occurs when the rotational stiffness is:

$$S_{r,opt} = \sqrt{\frac{8}{(1+\eta_r^2)}}k_b D. \quad \text{(29)}$$

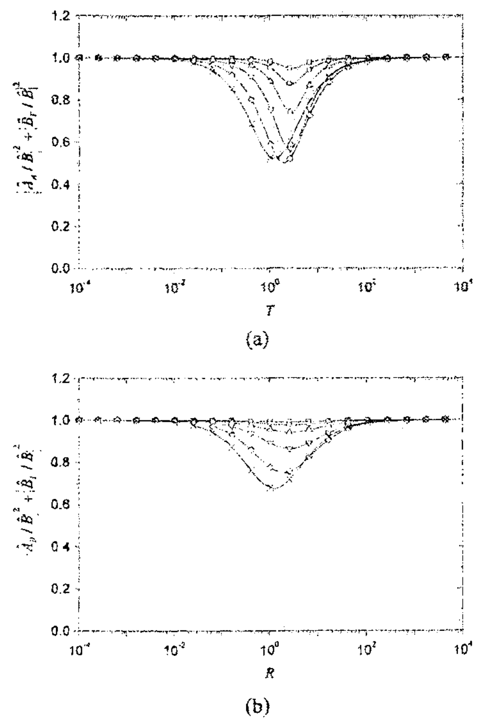

Fig. 5. Reflection ratio, $|\hat{A}_R/\hat{B}|^2 + |\hat{B}_T/\hat{B}|^2$, vs. non-dimensional stiffness parameters at the middle of the plate. (a) Effects of translational stiffness for R=0; (b) effects of rotational stiffness for T=0. Loss factors, η_t and η_r: , 0.023; , 0.06; , 0.15; , 0.4; , 1; , 2.

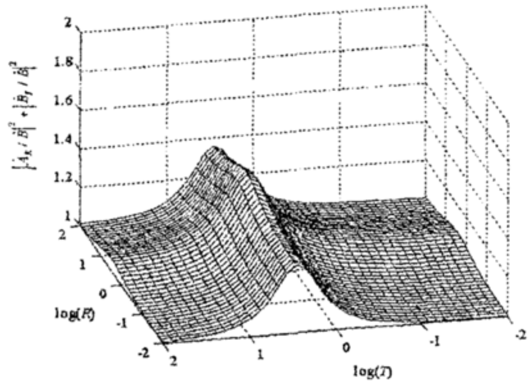

Fig. 6. Effects of the non-dimensional stiffness parameters on the inverse reflection and transmission ratio. $\eta_t=\eta_r=0.15$.

Similarly to the case of the translational stiffness, the optimal stiffness calculated from Eq. (29) is four times the stiffness that induces maximum dissipation of the incident waves at the edge. Fig. 5(b) shows the reflection ratio. The minimum value depends on the value of the loss factor at the edge. For the rotational stiffness, dissipation of incident waves increases as the loss factor increases when the rotational stiffness is optimum as shown in Fig. 5(b).

When the plate is supported by translational and rotational viscoelastic elements, Fig. 6 shows the variation of reflection ratio on the translational and rotational stiffness. Although the loss factor of the support stiffness is assumed to be the same value as the case of the stiffness at the edge, less dissipation of incident wave occurs in general. The saddle point observed for the support at the edge [6] does not occur in this case. The effects from the rotational and translational support stiffnesses are almost independent of each other.

4. Conclusions

Structural wave propagation was investigated in order to study the characteristics of dissipation at the supports. The support impedance that induces non-reflecting (impedance-matched) boundary conditions was obtained. This impedance was the same as the characteristic mechanical impedance of the supported structure. Also, the boundary impedance that minimized reflection and transmission at the compliant supports and tuned vibration absorber was calculated from which the optimal stiffness for maximum vibration energy dissipation was determined. The optimal impedance minimized reflection and transmission of structural waves from boundaries, and consequently reduces resonant response of the structure. When the support properties were viscoelastic, its stiffness was obtained assuming constant loss factor. A larger value of the stiffness is required when the supports are installed in the middle of the structure compared to the case of the edge supports. The calculation was related to wavenumber and structural properties, and can guide the design of supporting methods conveniently since it is done by simple closed form expression.

References

[1] J. C. Snowdon, Vibration and Shock in Damped Mechanical Systems, John Wiley & Sons, New York, USA, (1968).

[2] W. Soedel, Vibrations of Shells and Plates, Marcel Dekker, Inc., New York, USA, (1993).

[3] K.-H. Kang and K.-J. Kim, Modal properties of beams and plates on resilient supports with rotational and translational complex stiffness, *Journal of Sound and Vibration.* 190 (1996) 207-220.

[4] J. C. Macbain and J. Genin, Energy dissipation of a vibrating Timoshenko beam considering support and material damping, *International Journal of Mechanical Science.* 17 (1975) 255-265.

[5] G. Chen and J. Zhou, Vibration and Damping in Distributed Systems, Volume II: WKB and Wave Methods, Visualization and Experimentation. Boca Raton, CRC Press Inc., Florida, USA, (1993).

[6] J. Park, L. Mongeau and T. Siegmund, Influence of support properties on the forced vibrations of rectangular plates, *Journal of Sound and Vibration.* 264 (2003) 775-794.

[7] F. Fahy, Sound and Structural Vibration: Radiation, Transmission and Response, Academic Press, London, UK, (1985).

[8] J. D. Ferry, Viscoelastic Properties of Polymers. John Wiley & Sons, New York, USA, (1980).